Development 137, 3785-3794 (2010) doi:10.1242/dev.051805

Changes in the nuclear deposition of histone H2A variants during pre-implantation development in mice

Buhe Nashun[1], Masashi Yukawa[1], Honglin Liu[1,2], Tomohiko Akiyama[1] and Fugaku Aoki[1,*]

SUMMARY

Histone H2A has several variants, and changes in chromatin composition associated with their replacement might involve chromatin structure remodeling. We examined the dynamics of the canonical histone H2A and its three variants, H2A.X, H2A.Z and macroH2A, in the mouse during oogenesis and pre-implantation development when genome remodeling occurs. Immunocytochemistry with specific antibodies revealed that, although H2A and all variants were deposited in the nuclei of full-grown oocytes, only histone H2A.X was abundant in the pronuclei of one-cell embryos after fertilization, in contrast with the low abundance of histone H2A and the absence of H2A.Z. The decline in H2A and the depletion of H2A.Z and macroH2A after fertilization were confirmed using Flag epitope-tagged H2A, H2A.Z and macroH2A transgenic mouse lines. Microinjection experiments with mRNA encoding the Flag-tagged proteins revealed a similar pattern of nuclear incorporation of the H2A variants. Fusion protein experiments using H2A, H2A.Z and macroH2A fused with the C-terminal 23 amino acids of H2A.X showed that the C-terminal amino acids of H2A.X function specifically to target this variant histone into chromatin in embryos after fertilization and that the absence of H2A.Z and macroH2A from the chromatin is required for normal development. These results suggest that global changes in the composition of histone H2A variants in chromatin play a role in genome remodeling after fertilization.

KEY WORDS: H2A variants, Pre-implantation embryo, Epigenetics, Reprogramming, Mouse

INTRODUCTION

Histones are the main structural proteins that package eukaryotic DNA into chromatin. Although post-translational modification of histones and ATP-dependent remodeling are two major mechanisms that alter chromatin structure (Bernstein and Hake, 2006; Zlatanova and Thakar, 2008), it has been suggested that changes in nucleosome composition that occur as a result of the replacement of canonical histones with their variants also play important roles in chromatin remodeling (Ausio, 2006; Bernstein and Hake, 2006; Redon et al., 2002). A variety of variants for histones H2A, H2B and H3 have been identified in eukaryotes. Among these, histone H2A has the largest number of variants, including H2A.Z, H2A.X, macroH2A and H2A.Bbd, which are distinguished from the canonical H2A by variations in the length and sequence of their C-terminal tails (Kamakaka and Biggins, 2005; Pusarla and Bhargava, 2005).

One of the best-studied H2A variants is H2A.Z, which is highly conserved across species and is essential for the viability of various organisms (Zlatanova and Thakar, 2008). Allis et al. first suggested that H2A.Z is involved in transcriptional activation (Allis et al., 1980). A study in yeast demonstrated that H2A.Z acts as an anti-silencing factor at heterochromatin boundaries (Meneghini et al., 2003). Recently, it has been suggested that H2A.Z is involved in epigenetic memory (Brickner et al., 2007). H2A.X is another highly conserved histone variant (Redon et al., 2002). The major H2A proteins in yeast are more similar to the mammalian H2A.X variant than to the canonical H2A (Kamakaka and Biggins, 2005). One of the distinguishing characteristics of histone H2A.X is its C-terminal domain, which contains one or more SQ motifs. In response to DNA damage or DNA double-strand breaks, H2A.X is phosphorylated on a serine residue in its SQ motif, yielding a phosphorylated form of the protein known as γ-H2A.X (Rogakou et al., 1998). γ-H2A.X interacts with several DNA repair proteins, indicating that it is involved in the DNA repair process (Fernandez-Capetillo et al., 2004). MacroH2A is a vertebrate-specific histone variant that contains a large non-histone (NHR) C terminus and an N-terminal H2A-like region (Chadwick and Willard, 2001). The inactive X chromosome of female mammals is preferentially enriched with macroH2A, suggesting a role in X-chromosome inactivation (Costanzi and Pehrson, 1998). However, no significant differences in expression are observed between male and female cells (Rasmussen et al., 1999), suggesting that macroH2A might perform other functions in addition to the inactivation of the X chromosome.

During fertilization and pre-implantation development, the cells switch from terminally differentiated germ cells to undifferentiated totipotent zygotes and begin to differentiate at the late pre-implantation stage (Yamagata, 2008). During this period, the gene expression pattern changes substantially (Hamatani et al., 2004). This change is caused by genome-wide chromatin remodeling, which involves epigenetic reprogramming. In mammals, DNA methylation and histone modification are the two major epigenetic alterations (Morgan et al., 2005). Histone modifications in early embryos have been studied extensively in recent years (Fulka et al., 2008; Santos and Dean, 2004). However, to understand better the reprogramming that occurs during mammalian oogenesis and embryogenesis, the histone components that are the basic architectural proteins of the chromatin need to be defined throughout this entire process.

[1]Department of Integrated Biosciences, Graduate school of Frontier Sciences, University of Tokyo, Kashiwa, Chiba 277-8562, Japan. [2]College of Animal Science and Technology, Nanjing Agricultural University, Nanjing, 210095, China.

*Author for correspondence (aokif@k.u-tokyo.ac.jp)

Accepted 12 September 2010

In this study, we characterized chromatin incorporation and deposition of the canonical histone H2A (*Hist3h2a* – Mouse Genome Informatics) and its variants H2A.Z (*H2afz* – Mouse Genome Informatics), H2A.X (*H2afx* – Mouse Genome Informatics) and macroH2A (*H2afy* – Mouse Genome Informatics) in mouse oocytes and early embryos. We found that all of these histone H2A species were abundantly incorporated and deposited into chromatin in full-grown oocytes. However, with the exception of H2A.X, minimal, or no, incorporation of these proteins was observed during the early pre-implantation stage after fertilization; H2A.X exhibited significant incorporation during this period. These results suggest that global changes in chromatin structure, associated with altered histone composition, are involved in genome remodeling after fertilization.

MATERIALS AND METHODS

Collection of oocytes and embryos

Fully grown oocytes were collected from the ovaries of 8- to 12-week-old BDF1 mice (SLC, Japan) as described previously (Inoue and Aoki, 2010). The oocytes were arrested at germinal vesicle (GV) stage in medium containing 3-isobutyl-1-methylxanthine (IBMX). Metaphase (M) II-stage oocytes were collected from the oviducts of 3-week-old BDF1 mice and fertilized in vitro as described previously (Inoue and Aoki, 2010). The fertilized oocytes were cultured in KSOM medium. For immunocytochemical analysis, the embryos at the one-cell, two-cell, four-cell, morula and blastocyst stages were collected 12, 28, 45, 70 and 96 hours after insemination, unless otherwise specified.

Plasmid construction

The coding regions of histone H2A, H2A-614 (*Hist2h2aa2* – Mouse Genome Informatics), H2A.Z, macroH2A1.2 (*H2afy* – Mouse Genome Informatics), H2A.X, H2B (*Hist1h2bc* – Mouse Genome Informatics), and H4 (*Hist1h4a* – Mouse Genome Informatics) were PCR-amplified from total cDNA from full-grown oocytes or blastocyst-stage embryos. A Flag epitope tag and a linker sequence (GGsGG) were added to the N termini of the histone cDNAs by PCR amplification. C-terminus-deleted mutant versions of Flag-H2A.X and Flag-H2A.Z were amplified by PCR from the corresponding full-length sequences. The C-terminal 23 amino acid sequence of H2A.X was added to the C termini of Flag-H2A, Flag-H2A.Z, Flag-macroH2A and C-terminus-deleted Flag-H2A.Z in two PCR runs using primers containing sequences encoding the first half of this 23 amino acid sequence in the first run and others encoding the second half in the second run. The C-terminal 6 amino acids of H2A.Z were added to the C terminus of C-terminus-deleted H2A.X by PCR amplification performed using primers containing this 6 amino acid sequence. PCR products were cloned into the pCRII-TOPO vector using a TOPO TA Cloning Kit (Invitrogen) according to the manufacturer's instructions. All constructs were verified by DNA sequencing.

In vitro mRNA synthesis and microinjection

In vitro mRNA synthesis and microinjections were performed as described previously (Inoue and Aoki, 2010). Briefly, plasmids were linearized by appropriate restriction enzymes. Then 5′-capped mRNAs were synthesized and poly(A) tails were added. Finally, the DNA template was removed and synthesized mRNA was extracted. Approximately 10 pl synthetic RNA (~300 μg/ml) was microinjected into the cytoplasm of oocytes and embryos.

Production of transgenic mice carrying the Flag-tagged histone H2A variant genes

The pCAGGS vector (Niwa et al., 1991) was used to generate CAG promoter-driven Flag-H2A, Flag-H2A.Z and Flag-macroH2A transgenic mice. The pCRII-TOPO vectors encoding Flag-tagged histones were used to amplify the cDNA using *Eco*RI site-anchored primers and were then cloned into the *Eco*RI site of the pCAGGS vectors. These plasmids were double digested using *Hind*III and *Pvu*I to release the transgene cassette and were then microinjected into the pronucleus of one-cell embryos. Injected embryos were cultured to the two- or four-cell stage and transferred into the oviducts of pseudopregnant mice. Founder animals were screened by genotyping PCR.

Immunocytochemistry

Oocytes and embryos were fixed by incubating at room temperature for 40 minutes in PBS containing 3.7% paraformaldehyde and 0.2% Triton X-100. After washing with PBS containing 1% BSA, the cells were incubated with primary antibodies at 4°C overnight and then with secondary antibodies for 1 hour at room temperature. The primary antibodies used were: anti-H2A (MBL, D210-3; 1:300), anti-H2A.Z (Abcam, ab4174; 1:100), anti-H2A.X (Abcam, ab11175; 1:100), anti-Oct3/4 (Santa Cruz, sc-5279; 1:100) and anti-Flag (Sigma-Aldrich, F2555; 1:100). For oocytes or embryos obtained from transgenic mice or microinjected with Flag-tagged H2A variant mRNA, an anti-Flag M2 mouse monoclonal antibody (Sigma-Aldrich, F1804; 1:100) was used as the primary antibody. Alexa Fluor 488-conjugated anti-mouse IgG (Molecular Probes, A110011; 1:100) and FITC-conjugated anti-rabbit IgG (Jackson ImmunoResearch, 711-095-152; 1:100) were used as secondary antibodies. Alexa Flour 488- and 568-conjugated secondary antibodies were used for triple staining with anti-Flag and anti-Oct3/4 antibodies. DNA was stained for 30 minutes with 3 μg/ml 4,6-diamidimo-2-phenylindole (DAPI) and the cells were then mounted with Vectashield anti-bleaching solution (Vector Laboratories) on glass slides. Fluorescence was detected using a Carl Zeiss LSM510 laser-scanning confocal microscope. Semi-quantitative analysis of fluorescence signals was conducted using NIH image software, as described previously (Liu et al., 2004). All experiments were repeated at least three times (with the exception of those involving Flag-H2B and Flag-H4, which were performed twice), and approximately ten oocytes or embryos were analyzed in each replicate.

Measurement of blastocyst cell number

The embryos were collected 90 hours after insemination, subjected to hypotonic treatment for 20 minutes in 0.9% sodium citrate containing 0.3% polyvinylpyrrolidone, and then transferred to a mixture of methanol, acetic acid and sterilized water (5:1:4) to fix for 2 minutes. After fixation, embryos were adhered to a glass slide by dripping a mixture of methanol and acetic acid (3:1). Nuclear DNA was stained with DAPI and the number of nuclei was counted on a fluorescent microscope.

Immunoblotting

GV-stage oocytes and one-cell embryos were transferred into 3× SDS loading buffer. After denaturation for 3 minutes at 95°C, urea was added to give a final concentration of 8 M. Proteins were separated on 15% SDS gels and blotted as described previously (Inoue and Aoki, 2010). Anti-H2A.X (Abcam, ab11175; 1:1000), anti-H2A.Z (Millipore, 07594; 1:2000), and anti-α-tubulin (Sigma-Aldrich, T6074; 1:4000) primary antibodies were used.

Semi-quantitative reverse transcription (RT)-PCR

Twenty GV-stage oocytes or one-cell embryos were dissolved in ISOGEN (Nippon Gene), and RNA was isolated as described previously (Kageyama et al., 2007). Reverse transcription was performed with random primers using a Prime Script RT-PCR Kit (Takara). The primers used and thermal conditions employed for PCR are shown in Table S1 in the supplementary material.

RESULTS

Nuclear deposition of the canonical histone H2A decreases after fertilization

First, we examined the dynamics of the canonical histone H2A during oogenesis and pre-implantation development using a specific antibody. Histone H2A was detected in the GVs of full-grown oocytes and in the condensed chromosomes of mature MII-stage oocytes (Fig. 1A). After fertilization, the oocytes complete the second meiosis and then form the male and female pronuclei. At this stage, H2A was present in the two pronuclei but the fluorescent signal became weaker than that observed in GV-stage oocytes. During the following developmental stages, the signal was still weak

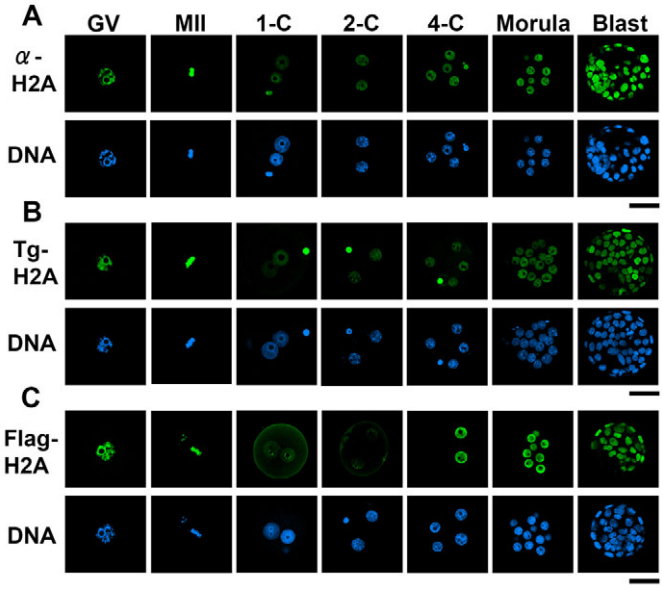

Fig. 1. Nuclear deposition and incorporation of the canonical histone H2A in mouse oocytes and pre-implantation embryos. (**A**) A specific antibody against H2A was used to detect the endogenous H2A protein in oocytes at the germinal vesicle (GV) and metaphase II (MII) stages, and in embryos at the one-cell (1-C), two-cell (2-C), four-cell (4-C), morula (Morula) and blastocyst (Blast) stages. (**B**) Flag-H2A was detected in the oocytes and embryos of Flag-H2A transgenic mice using an anti-Flag antibody. (**C**) Nuclear incorporation of Flag-H2A was examined by microinjecting mRNA encoding Flag-H2A. In the analysis of late pre-implantation embryos, mRNA was microinjected into only one blastomere of each two-cell embryo. Therefore, the Flag-H2A signal was detected in only half of the nuclei in the four-cell, morula and blastocyst-stage embryos. DNA was stained with DAPI. Scale bars: 50 μm.

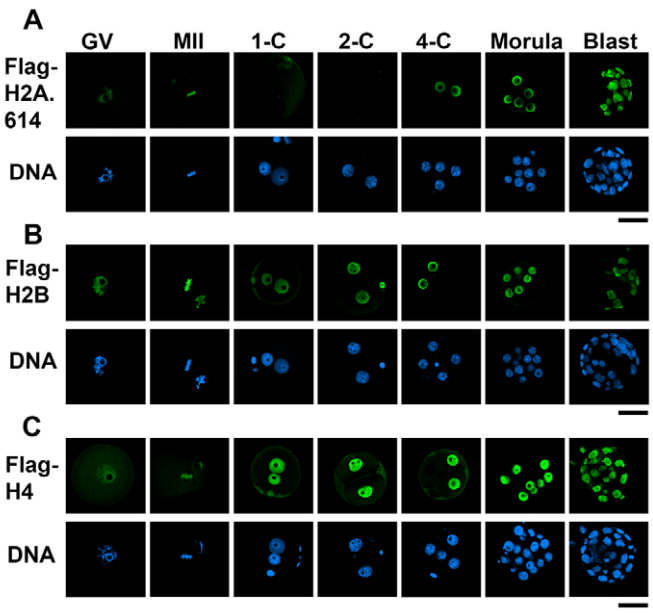

Fig. 2. Incorporation of Flag-tagged H2A-614, H2B and H4 into mouse oocytes and pre-implantation embryos. (**A-C**) Nuclear incorporation of Flag-tagged histones was examined in oocytes at the germinal vesicle (GV) and metaphase II (MII) stages, and in embryos at the one-cell (1-C), two-cell (2-C), four-cell (4-C), morula (Morula) and blastocyst (Blast) stages by microinjecting mRNA encoding Flag-H2A-614 (A), Flag-H2B (B) and Flag-H4 (C). In the analysis of late pre-implantation embryos, mRNA was microinjected into only one blastomere of each two-cell embryo. DNA was stained with DAPI. Scale bars: 50 μm.

in two-cell embryos but, thereafter, it gradually increased. A strong H2A signal comparable with that in GV-stage oocytes was observed in blastocysts. These results demonstrate that the level of canonical histone H2A was high in full-grown and mature oocytes, decreased after fertilization, and then increased up to the blastocyst stage.

To confirm the immunostaining data, we generated transgenic mice whose oocytes expressed Flag-tagged H2A, and investigated the changes in nuclear deposition of Flag-tagged H2A during oogenesis and pre-implantation development. The pattern of changes in nuclear deposition of Flag-tagged H2A was exactly the same as that observed for endogenous H2A detected using the specific antibody. Substantial Flag-H2A deposition was observed both in GVs and MII oocytes. It decreased after fertilization, remained at a low level until the two-cell stage and then gradually increased up to the blastocyst stage (Fig. 1B). We analyzed oocytes and embryos derived from three independent Flag-H2A transgenic lines and obtained comparable results in all of them. These results confirmed our observations using the H2A-specific antibody.

It is likely that these changes in H2A nuclear deposition were caused by changes in the rate of H2A incorporation into chromatin. To test this hypothesis, we microinjected Flag-tagged H2A mRNA into oocytes and embryos, and examined nuclear incorporation of the tagged protein. A strong Flag signal was observed in the GVs of full-grown oocytes injected with mRNA and maintained in IBMX-containing medium for 5 hours (Fig. 1C). A similar intensity of signal was observed in the chromosomes of MII-stage oocytes 14 hours after their release into IBMX-free medium. However, when MII-stage oocytes were injected with mRNA and then fertilized, only a weak signal was detected 12 and 28 hours post-insemination (hpi) in the pronuclei of one-cell embryos and the nuclei of two-cell embryos, respectively. We then injected the mRNA into one of two blastomeres in late two-cell embryos in order to analyze Flag-tagged histone H2A incorporation after the two-cell stage. An intense Flag-H2A signal was detected in the nuclei of embryos at the four-cell (45 hpi), morula (70 hpi) and blastocyst (96 hpi) stages, indicating that active incorporation of Flag-H2A into chromatin occurs at these stages. These data were consistent with those obtained using a specific antibody and from the transgenic mouse analysis. Taken together, these results suggest that the active incorporation of H2A maintains the high level of nuclear H2A in oocytes and four-cell and later-stage embryos, and that limited incorporation leads to a decline in nuclear H2A at the one- and two-cell stages.

The canonical histone H2A is encoded by at least 20 genes, the protein products of which differ only slightly (Marzluff et al., 2002). Therefore, we examined the nuclear incorporation of another H2A gene product, H2A-614, which has been reported to be abundantly transcribed in mouse oocytes (Graves et al., 1985). The results obtained were consistent with those for the canonical H2A gene (Fig. 2A). The Flag-tagged H2A-614 protein was incorporated into GVs and the chromosomes of MII-stage oocytes. Nuclear incorporation was almost undetectable in one-cell and two-cell embryos, but increased by the four-cell stage.

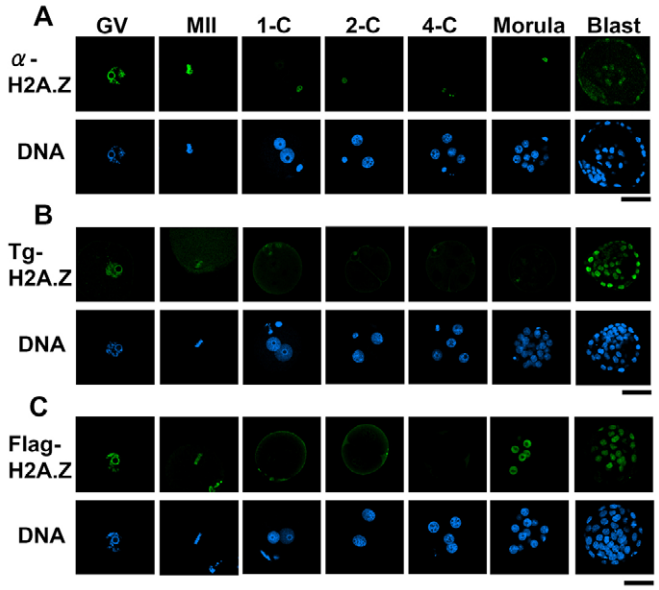

Fig. 3. Nuclear deposition and incorporation of H2A.Z in oocytes and pre-implantation embryos. (**A**) A specific antibody against H2A.Z was used to detect the endogenous H2A.Z protein in oocytes at the germinal vesicle (GV) and metaphase II (MII) stages, and in embryos at the one-cell (1-C), two-cell (2-C), four-cell (4-C), morula (Morula), and expanded blastocyst (Blast) stages. As the signal at blastocyst stage (96 hpi) was very weak, an image of the expanded blastocyst stage (120 hpi) is shown here. (**B**) Flag-H2A.Z was detected in the oocytes and embryos of Flag-H2A.Z transgenic mice using an anti-Flag antibody. (**C**) Nuclear incorporation of Flag-H2A.Z was examined by microinjecting mRNA encoding Flag-H2A.Z. In the analysis of late pre-implantation embryos, mRNA was microinjected into only one blastomere of each two-cell embryo. DNA was stained with DAPI. Scale bars: 50 μm.

We also investigated the nuclear incorporation of other core histones, H2B and H4, in mRNA microinjection experiments. Flag-tagged H2B and H4 proteins were constantly incorporated into chromatin in embryos throughout the pre-implantation stage (Fig. 2B,C) but H4 incorporation was lower in the oocytes than in the embryos.

Maternal H2A.Z is lost in nuclei after fertilization

Immunocytochemistry with a specific antibody revealed an intense H2A.Z signal in the GVs of full-grown oocytes and the chromosomes of MII-stage oocytes (Fig. 3A). However, the signal was absent in the pronuclei of one-cell embryos after fertilization and was not detected in the nuclei until the morula stage, although it remained in polar bodies. A very weak signal was detected at the blastocyst stage (96 hpi) and the signal intensity gradually increased thereafter until the expanded blastocyst stage (120 hpi). Removal of H2A.Z from chromatin seemed to occur gradually during the one-cell stage. The H2A.Z signal decreased but was still clearly detected in the female pronucleus at 3 hpi, was very weak at 6 hpi and was mostly lost at 12 hpi (see Fig. S1 in the supplementary material).

To validate the obtained results by specific antibody staining, we generated two independent transgenic mouse lines expressing Flag-H2A.Z. H2A.Z accumulated in the GVs of full-grown oocytes collected from transgenic female mice (Fig. 3B). The Flag-H2A.Z signal colocalized with that of DNA stained with DAPI throughout the GV stage, except for the DNA-dense heterochromatic regions (see Fig. S2A in the supplementary material). In MII-stage oocytes, an intense signal was still detected in the chromosomes; however, it was completely lost after fertilization and no signal was detected until the morula stage. When the detection intensity of the microscope was increased, only a faint Flag-H2A.Z signal was detected in the nuclei of embryos at the one-cell and morula stages and no signal was observed at the two- and four-cell stages (see Fig. S3A in the supplementary material). When embryos reached the blastocyst stage, the Flag-H2A.Z signal reappeared (Fig. 3B), as was observed in the specific H2A.Z antibody staining experiments (Fig. 3A). Similar patterns of H2A.Z deposition were observed in two different transgenic mouse lines. Because it was reported that H2A.Z was detected only in trophectoderm cells and not in inner cells (Rangasamy et al., 2003), we performed triple-staining experiments using an anti-Oct3/4 (Pou5f1 – Mouse Genome Informatics) antibody, which allows cells of the two lineages to be distinguished. The results clearly show that H2A.Z was deposited at higher levels in the nuclei of Oct3/4-negative trophectoderm cells than in those of Oct3/4-positive inner cells (see Fig. S4 in the supplementary material).

The results of the experiments described above, performed using a specific antibody and transgenic Flag-tagged H2A.Z mouse lines, suggest that H2A.Z is lost from the zygotic genome after fertilization. However, it is possible that H2A.Z was present, but that it was not detected because of a decrease in the accessibility of H2A.Z and Flag-tag epitopes to antibodies. To address this issue, we microinjected mRNA encoding EGFP-fused H2A.Z into GV-stage oocytes and monitored changes in EGFP fluorescence following fertilization. EGFP-H2A.Z was incorporated into GV chromatin, but the EGFP signal became very weak in the pronucleus following fertilization (see Fig. S5 in the supplementary material). No EGFP signal was detected in the nuclei of two-cell embryos. These results strongly suggest that H2A.Z is lost from the zygotic genome after fertilization.

It is likely that the disappearance of H2A.Z was caused by its limited or non-incorporation into chromatin after fertilization, as is the case with H2A. To test this, Flag-tagged H2A.Z mRNA experiments, similar to those performed for Flag-H2A, were conducted. Flag-H2A.Z was incorporated into the GVs of full-grown oocytes and the chromosomes of MII-stage oocytes (Fig. 3C). However, after fertilization, no incorporation was observed until the four-cell stage. When the detection intensity of the microscope was increased, only a faint Flag-H2A.Z signal was detected in the pronuclei and nuclei of one-cell and two-cell embryos, respectively, whereas stronger signals were detected in embryos that had been microinjected with Flag-H2A mRNA (see Fig. S6 in the supplementary material). Nuclear incorporation of Flag-H2A.Z was also detected in morula and blastocyst-stage embryos (Fig. 3C). Thus, the changes in H2A.Z nuclear incorporation could explain the changes in nuclear deposition before and after fertilization. H2A.Z accumulated in the GVs of full-grown oocytes because it was well incorporated. After fertilization, minimal H2A.Z incorporation caused its disappearance from the nuclei. At the morula stage, because its incorporation had only just commenced, H2A.Z had not yet greatly accumulated in the nuclei. Subsequent continuous incorporation resulted in the detection of accumulated H2A.Z at the blastocyst stage.

MacroH2A is absent from the nucleus in one- and two-cell embryos

Using a specific antibody, Chang et al. described the dynamics of macroH2A deposition in mouse oocytes and embryos (Chang et al., 2005). In the present study, Flag-macroH2A transgenic mouse lines were established to confirm those results. We detected strong macroH2A signals in both the GVs of full-grown oocytes and the

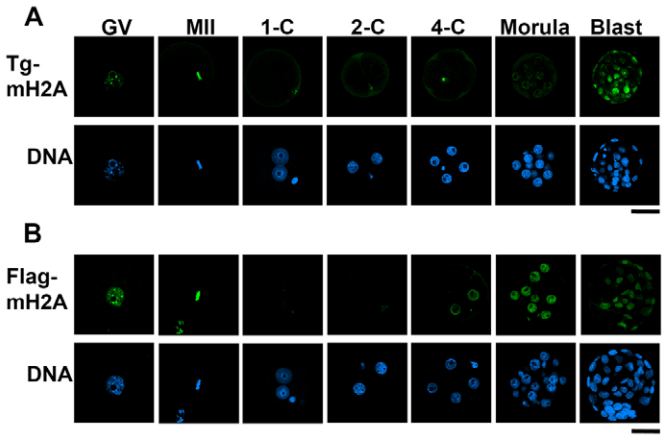

Fig. 4. Nuclear deposition and incorporation of macroH2A in mouse oocytes and pre-implantation embryos. (**A**) Flag-macroH2A transgenic mice (Tg-mH2A) were used to analyze macroH2A deposition in the nuclei of oocytes at the germinal vesicle (GV) and metaphase II (MII) stages, and of embryos at the one-cell (1-C), two-cell (2-C), four-cell (4-C), morula (Morula) and blastocyst (Blast) stages. (**B**) Nuclear incorporation of macroH2A was examined by microinjecting mRNA encoding Flag-macroH2A. In the analysis of late pre-implantation embryos, mRNA was microinjected into only one blastomere of each two-cell embryo. DNA was stained with DAPI. Scale bars: 50 μm.

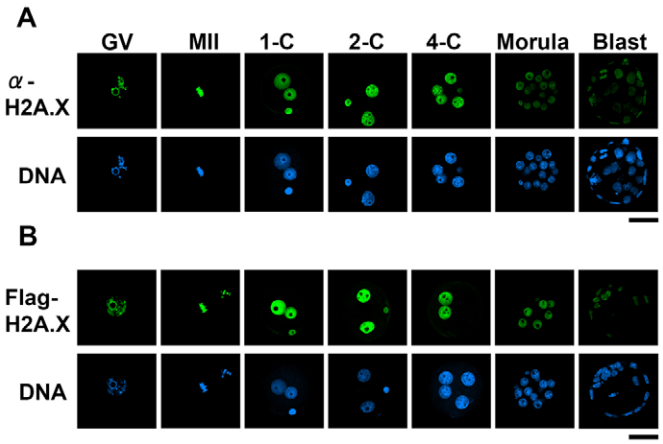

Fig. 5. Nuclear deposition and incorporation of H2A.X in mouse oocytes and pre-implantation embryos. (**A**) A specific antibody against H2A.X was used to detect endogenous H2A.X protein in oocytes at the germinal vesicle (GV) and metaphase II (MII) stages, and in embryos at the one-cell (1-C), two-cell (2-C), four-cell (4-C), morula (Morula) and blastocyst (Blast) stages. (**B**) Nuclear incorporation of Flag-H2A.X was examined by microinjecting mRNA encoding Flag-H2A.X. In the analysis of late pre-implantation embryos, mRNA was microinjected into only one blastomere of each two-cell embryo. DNA was stained with DAPI. Scale bars: 50 μm.

chromosomes of MII-stage oocytes obtained from transgenic females (Fig. 4A). In the GVs, the signals were concentrated in the DNA-dense heterochromatin regions (see Fig. S2A in the supplementary material). However, after fertilization, macroH2A signals decreased to very low or undetectable levels in the pronuclei of late one-cell embryos (with the exception of the polar bodies), even at an increased detection intensity (Fig. 4A; see Fig. S3B in the supplementary material). Signal was still not detected during the two- and four-cell stages. A weak signal was detected at the morula stage, and then its intensity increased at the blastocyst stage (Fig. 4A). These patterns of macroH2A deposition were observed in two different transgenic mouse lines. These results are consistent with those reported previously (Chang et al., 2005). Next, we conducted mRNA microinjection experiments to examine macroH2A nuclear incorporation, as were performed in the analyses of H2A and H2A.Z. The results showed that Flag-tagged macroH2A was incorporated into the GV chromatin and MII chromosomes (Fig. 4B). However, after fertilization, no further incorporation of macroH2A was observed in male or female pronuclei. At an increased detection intensity, only a very weak signal was detected (see Fig. S4C in the supplementary material). MacroH2A incorporation was still not detected at the two-cell stage, was detected weakly at the four-cell stage and increased gradually until the blastocyst stage (Fig. 4B), in agreement with the increased accumulation of macroH2A at this stage in transgenic mouse embryos (Fig. 4A). The kinetics of macroH2A deposition and incorporation were thus similar to those of H2A.Z, although the time at which deposition and incorporation were detected for the first time after fertilization was slightly earlier for macroH2A than H2A.Z.

H2A.X is enriched in early pre-implantation embryos

Immunocytochemistry with a specific antibody revealed that H2A.X is the only H2A variant deposited abundantly in the nuclei of one- and two-cell embryos (Fig. 5A). H2A.X was deposited in the GVs of full-grown oocytes and the chromosomes of MII-stage oocytes. In contrast to H2A, H2A.Z and macroH2A, an intense H2A.X signal was detected after fertilization in both male and female pronuclei. At the two- and four-cell stages, the signal intensity remained higher than that in GV-stage oocytes; however, it decreased at the morula stage and further at the blastocyst stage.

The mRNA microinjection experiments with a Flag-tagged protein showed that active H2A.X incorporation occurs during early pre-implantation development. A higher Flag-H2A.X signal intensity was observed in one-cell embryos (Fig. 5B). The signals remained intense at the two- and four-cell stages and then decreased at the morula stage. These results suggest that active incorporation of H2A.X results in its abundant deposition in the nuclei in early pre-implantation embryos.

It is known that protamine-histone exchange occurs in the paternal genome within 2 hours of fertilization (van der Heijden et al., 2005). To confirm that H2A.X is incorporated during this process, Flag-H2A incorporation was closely observed at 1-hour intervals post-fertilization (see Fig. S7 in the supplementary material). One hour after insemination, Flag-H2A.X was not yet incorporated into the paternal genome, although it was already detected in condensed maternal chromosomes. Because Flag-H2A.X was injected into oocytes 2 hours before insemination, most of the Flag-H2A.X deposited on maternal chromosomes at this time point would have been incorporated prior to fertilization. From 2-4 hours post-insemination, the signal of Flag-H2A.X was stronger in the paternal genome than in the maternal one.

Quantitative analysis of H2A variants in M phase chromosomes

As described above, nuclear levels of the histone variants changed drastically after fertilization. These changes in histone abundance in the nucleus should mirror those in the chromatin, as it has been reported that more than 90% of histones in the cell are incorporated into chromatin, and that the free nuclear histone fraction is very

small (Loyola et al., 2006). However, because oocytes and embryos before the four-cell stage contain large maternal free histone pools (Wassarman and Mrozak, 1981), the possibility cannot be excluded that there are significant amounts of free histone proteins in the nucleoplasm of oocytes and that their abundance in the nucleus does not reflect that in chromatin. Therefore, to confirm that the levels of chromatin-associated histones changed rather than just their nuclear abundance, we quantified the histone variants in metaphase chromatin of oocytes and embryos before the four-cell stage. Levels of histone variants were assessed semi-quantitatively by measuring the immunofluorescence signal intensity obtained using each specific antibody relative to the DNA content (determined by measuring DAPI fluorescence). Levels of H2A in the one- and two-cell embryos were nearly half of that in oocytes that had undergone germinal vesicle break down (GVBD) (Fig. 6). The amount of H2A.Z in one-cell embryos was less than 20% of that in the oocytes. H2A.Z was not detected in the M-phase chromosomes of two-cell embryos. By contrast, the amount of H2A.X increased significantly after fertilization. These data indicate that the abundance of histones in the nucleus reflect those in the chromatin in oocytes and early pre-implantation embryos.

The C-terminal 23 amino acids of H2A.X are responsible for its incorporation into chromatin after fertilization

Histone H2A.X is composed of 143 amino acids and is 13 and 15 amino acids longer than histone H2A and H2A.Z, respectively. The amino acid sequences of these three proteins are similar in their N-terminal regions (120 amino acids in H2A and H2A.X, 122 amino acids in H2A.Z), which end with two successive lysine residues, but they are very different from each other in terms of their C-terminal residues (Fig. 7A). The N-terminal region contains the histone fold domain, which is involved in nucleosome formation, but the role of the C terminus is not fully understood. As described above, histone H2A and H2A.Z were rarely incorporated into the chromatin after fertilization (Fig. 1C and Fig. 3C), whereas H2A.X was abundantly incorporated (Fig. 5B). Therefore, we speculated that the H2A.X sequences following residue 120 might play a role in H2A.X incorporation into chromatin after fertilization.

To test this hypothesis, we deleted the C-terminal 23 amino acids from H2A.X to create a construct encoding the N-terminal region of H2A.X fused with a Flag-tag (H2A.XΔC). When MII-stage oocytes were microinjected with H2A.XΔC mRNA and then fertilized, only a weak Flag signal was detected in the nuclei of one- and two-cell embryos. Indeed, its signal intensity was much lower than that of intact H2A.X (Fig. 7B). The level of nuclear incorporation was also low when the N-terminal region of H2A.X was fused with the C-terminal six amino acids of H2A.Z (H2A.XΔC-ZC6). Next, we deleted the C terminus from H2A.Z (ZC6) and replaced it with the C terminus of H2A.X (XC23), thereby generating the chimeric protein H2A.ZΔC-XC23. Although neither intact nor C-terminus-deleted (H2A.ZΔC) H2A.Z was incorporated into the nuclei of one-cell or two-cell embryos, H2A.ZΔC-XC23 was abundantly incorporated at a level comparable with that of H2A.X (Fig. 7C). Active incorporation was also observed when the C terminus of H2A.X was directly fused to the C terminus of intact H2A.Z (H2A.Z-XC23). Furthermore, the chimeric proteins H2A-XC23 and macroH2A-XC23, formed by the fusion of H2A and macroH2A, respectively, with the C terminus of H2A.X, were abundantly incorporated into the nucleus after fertilization, although the wild-type forms, H2A and macroH2A, were not (Fig. 7D,E). These results suggest that the C-terminal 23 amino acids of H2A.X are responsible

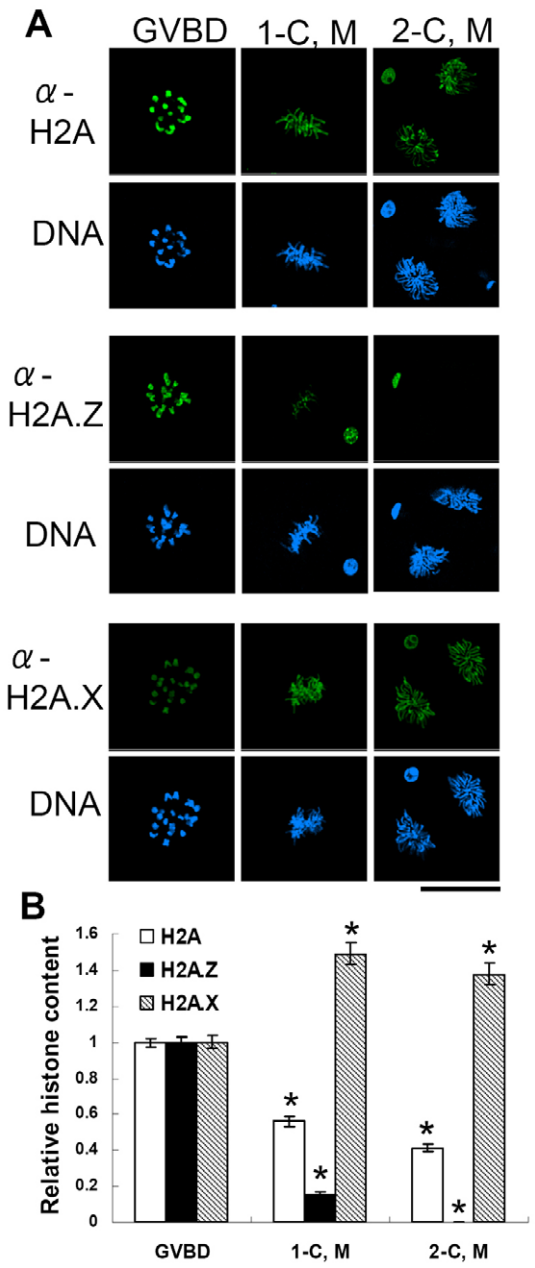

Fig. 6. Levels of chromatin-deposited histones at the M phase of the cell cycle in mouse oocytes and early pre-implantation embryos. (**A**) Representative images of oocytes and embryos immunostained with antibodies against H2A, H2A.Z and H2A.X. Oocytes were collected during germinal vesicle breakdown (GVBD) 3 hours after being transferred to IBMX-free medium, and one-cell and two-cell embryos at the M phase (1-C,M and 2-C,M, respectively) were collected approximately 14 and 37 hours after insemination, respectively. These cells were simultaneously stained for comparison. DNA was stained with DAPI. Scale bar: 50 μm. (**B**) Quantitative analysis of fluorescence intensities. Histone and DNA fluorescent signals were measured as described in the Materials and methods, and the ratio of histone to DNA was determined. The mean value for oocytes in each experiment was set at 1, and relative values for all other samples were calculated accordingly. The experiments were performed three times, and 8-14, 5-12 and 11-16 cells were analyzed in each experiment for H2A, H2A.Z and H2A.X signals, respectively. Asterisks indicate significant differences ($P<0.001$) versus oocytes (Student's *t*-test). Error bars represent s.e.m.

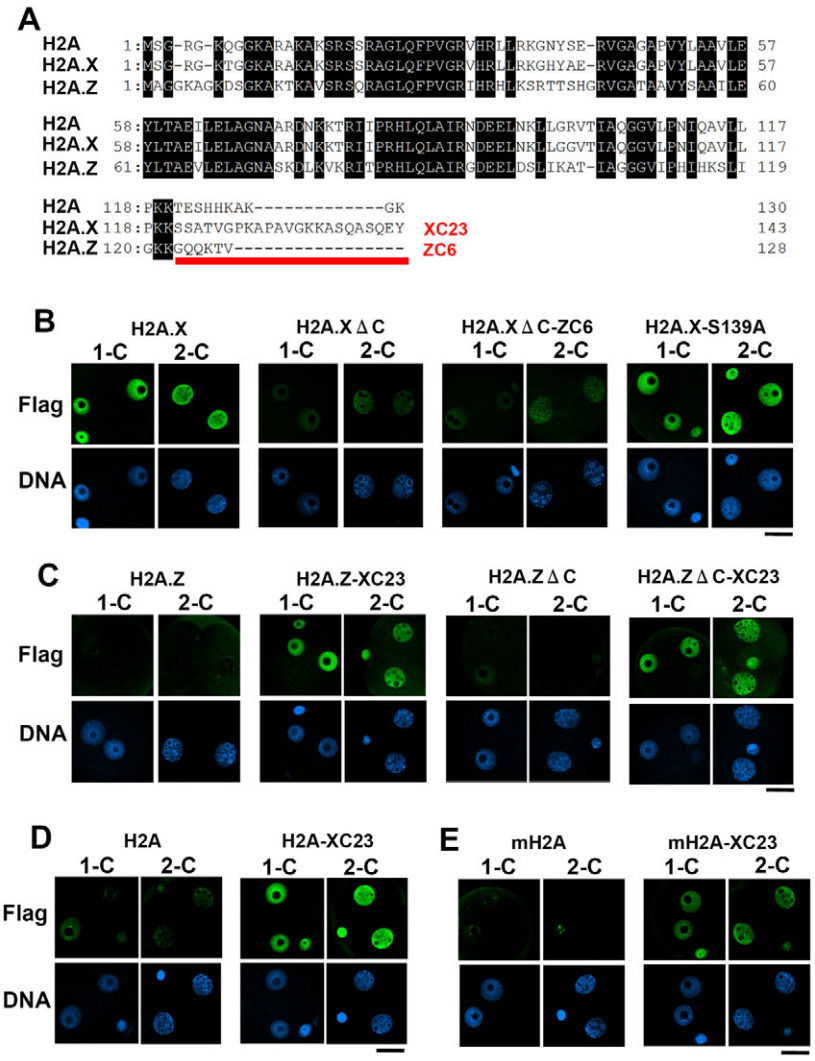

Fig. 7. The C-terminal 23 amino acids are responsible for H2A.X chromatin incorporation after fertilization. (**A**) Amino acid sequence alignment for mouse histone H2A, H2A.X and H2A.Z. In the alignment, amino acids that are identical in all three proteins are highlighted. The red line indicates the C-terminal domains used for the fusion experiments. (**B**) The C-terminal 23 amino acids of H2A.X were deleted (H2A.XΔC) or replaced with the C-terminal six amino acids of H2A.Z (H2A.XΔC-ZC6). A plasmid encoding a mutant form of H2A.X, in which Ser139 is replaced with an alanine residue (H2A.X-S129A), was also constructed. The mRNAs encoding these modified proteins (all Flag-tagged) were microinjected into metaphase II-stage oocytes. The oocytes were inseminated 2 hours after microinjection and collected at the one-cell (1-C) and two-cell stages (2-C) at 6 and 28 hours post-insemination, respectively, for immunocytochemical analyses using an anti-Flag antibody. (**C**) The C-terminal six amino acids of H2A.Z were deleted (H2A.ZΔC) or replaced with the C-terminal 23 amino acids of H2A.X (H2A.ZΔC-XC23). A plasmid encoding a chimeric form of H2A.Z, in which the C terminus of H2A.X was directly fused to the C terminus of intact H2A.Z (H2A.Z-XC23), was also constructed. mRNAs encoding these modified proteins were microinjected into metaphase II-stage oocytes, as described in B and analyzed using an anti-Flag antibody. (**D**,**E**) mRNAs encoding the fusion proteins H2A-XC23 (D) and mH2A-XC23 (E), in which H2A and macroH2A are respectively fused to the C terminus of H2A.X, were microinjected into metaphase II-stage oocytes, as described in B and analyzed using an anti-Flag antibody. DNA was stained with DAPI. Scale bars: 20 μm.

for its active chromatin incorporation after fertilization. Finally, to examine whether the phosphorylation of Ser139 is important for H2A.X incorporation, we replaced this amino acid with an alanine residue. The resulting H2A.X mutant was abundantly incorporated into chromatin (Fig. 7B), suggesting that the phosphorylation of H2A.X at Ser139 is not required for its incorporation into chromatin.

Incorporation of H2A.Z-XC23 and macroH2A-XC23 into chromatin after fertilization has a detrimental effect on developmental progression

To investigate the effect of H2A.Z-XC23 nuclear incorporation on development, MII-stage oocytes were microinjected with H2A.Z-XC23, H2A.X or H2A.Z mRNA, and their developmental rates were examined after fertilization. Although ~90% of the embryos that had been microinjected with H2A.X or H2A.Z mRNA cleaved into two-cell embryos at 17 hpi, only 66% of H2A.Z-XC23 mRNA-microinjected embryos cleaved (Fig. 8A). The embryos that had not cleaved at 17 hpi were not arrested at the one-cell stage but seemed to be delayed in their development, because the percentage of cleaved embryos increased to ~90% at 24 hpi. This delay in the early phase of development affected the rate of development to the blastocyst stage. Only 62% of embryos that had been microinjected with H2A.Z-XC23 mRNA developed to the blastocyst stage, whereas ~90% of the embryos microinjected with H2A.X or H2A.Z mRNA did (Fig. 8B). Even in the embryos that had developed into blastocysts, the number of cells was significantly lower in the H2A.Z-XC23 mRNA-microinjection group than in the other ones (Fig. 8C). Thus, H2A.Z-XC23 incorporation into chromatin has a detrimental effect on developmental progression. The nuclear incorporation of macroH2A-XC23 also showed similar effects on pre-implantation development (Fig. 8D,E,F). These results suggest that the absence of H2A.Z and macroH2A from the chromatin in early pre-implantation embryos is required for normal development.

DISCUSSION

Histone H2A and its variants are actively exchanged (Higashi et al., 2007), and the equilibrium between their removal and incorporation determines their abundance in chromatin. The decrease in H2A, H2A.Z and macroH2A deposition in the nucleus after fertilization might have been caused by a decrease in the incorporation rate of these proteins into chromatin; H2A.Z and macroH2A were almost completely lost from the nucleus owing to their weak incorporation, and a low level of H2A was present in the nucleus because it was still incorporated in chromatin at a low level. Alternatively, it is possible that the amount of these variant proteins stored in oocytes changes after fertilization, leading to changes in the level of nuclear deposition. To address this hypothesis, we examined the expression

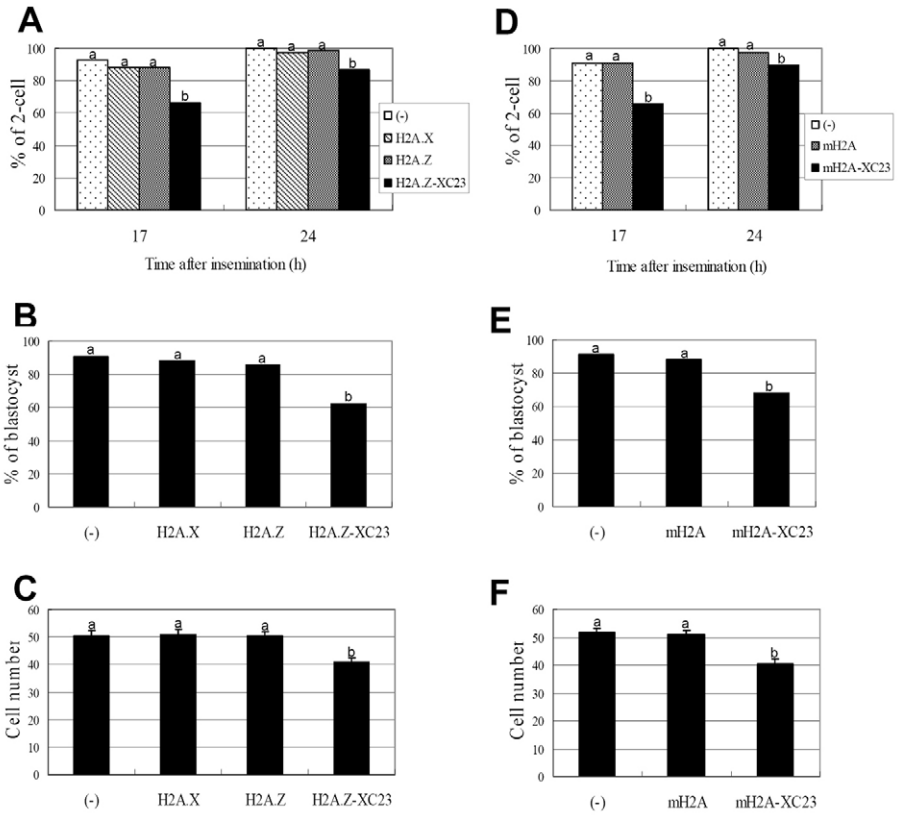

Fig. 8. Nuclear incorporation of forms of histone H2A.Z and macroH2A carrying H2A.X C-terminal amino acids causes developmental delay. (**A-F**) Metaphase II-stage mouse oocytes were microinjected with mRNA encoding Flag-tagged H2A.X, H2A.Z, mH2A, H2A.Z-XC23 or mH2A-XC23 and inseminated 2 hours later. (A,D) The percentage of embryos that developed to the two-cell stage was determined 17 and 24 hours after insemination. (B,E) The percentage of embryos that had developed to the blastocyst stage were examined 90 hours after insemination. (C,F) The number of cells in the blastocysts were counted. In A, B, D and E, three or more independent experiments were performed, and at least 77 embryos were analyzed in each group. In C and F, data represent the mean ± s.e.m. of three independent experiments. At least 22 embryos were analyzed in each group. Significant difference (a versus b; $P<0.01$) was determined by the χ^2 test (B,E, 17 hours in A and D), Fisher's exact test (24 hours in A and D) or Student's *t*-test (C,F).

of histone H2A and its variants by RT-PCR. However, these transcripts were expressed at similar levels before and after fertilization (see Fig. S8A in the supplementary material). Furthermore, in immunoblotting analyses performed using anti-H2A.X and anti-H2A.Z antibodies, levels of histone proteins changed little after fertilization (see Fig. S8B,C in the supplementary material). Thus, the mechanisms regulating the rates of H2A variant incorporation might instead be dramatically altered after fertilization. It is also likely that there is some mechanism to actively remove H2A.Z and macroH2A from the chromatin in early pre-implantation embryos because the rates of their disappearance were higher than that of H2A. In photobleaching experiments, Kimura and Cook found that histone H2B, which is the tightest counterpart of histone H2A, took ~6 hours to recover to 50% of its pre-photobleaching level (Kimura and Cook, 2001), suggesting that half of the histone H2B in the photobleached region was exchanged during this time period. However, our analyses using specific antibodies showed that the histone H2A.Z signal became very weak 6 hours after insemination (see Fig. S1 in the supplementary material). Chang et al. similarly demonstrated that macroH2A disappeared 7 hours after fertilization (Chang et al., 2005). Therefore, proteins that recognize specific H2A.Z and macroH2A sequences might promote their removal after fertilization.

In *Xenopus*, H2A.X is incorporated into sperm chromatin following fertilization (Dimitrov et al., 1994; Ohsumi and Katagiri, 1991). Here, we demonstrated for the first time that, in mammals, H2A.X is abundantly incorporated into the paternal genome soon after fertilization (see Fig. S7 in the supplementary material). During mammalian spermatogenesis, a histone-to-protamine exchange occurs and the DNA becomes highly condensed (Kimmins and Sassone-Corsi, 2005). However, soon after fertilization, the protamines are rapidly removed and replaced by nucleosomal histones (Kimmins and Sassone-Corsi, 2005; van der Heijden et al., 2005). H2A.X was incorporated more slowly into the female genome than into the male genome (see Fig. S7 in the supplementary material). This might be because H2A.X replaces H2A.Z and macroH2A, which are gradually removed after fertilization (see Fig. S1 in the supplementary material) (Chang et al., 2005)

Extensive genome reprogramming occurs soon after fertilization (Morgan et al., 2005; Santos and Dean, 2004), and changes in the deposition of H2A variants might be involved in this process. We have shown that H2A.Z and macroH2A are rapidly lost from chromatin soon after fertilization. When H2A.Z and macroH2A carrying the C terminus of H2A.X were incorporated into chromatin following fertilization, pre-implantation development was retarded (Fig. 8). The absence of these proteins might be necessary for genome reprogramming after fertilization. Angelov et al. suggested that macroH2A-containing nucleosomes are resistant to chromatin remodeling (Angelov et al., 2003). Thus, it is possible that the disappearance of macroH2A following fertilization allows the chromatin to be easily remodeled (Santenard and Torres-Padilla, 2009). Brickner et al. reported that H2A.Z acts as a form of epigenetic memory for transcriptionally active genes (Brickner et al., 2007) and, more recently, Jin et al. demonstrated that insulator regions are enriched with H2A.Z (Jin et al., 2009). Thus, the removal of histone H2A.Z after fertilization might erase the previous transcriptional memory and eliminate the insulator regions, which could be important during genome reprogramming.

Throughout the life cycle, the genome is extensively reprogrammed twice, i.e. during gametogenesis and pre-implantation development (Morgan et al., 2005), and similar epigenetic changes have been observed during these periods. In mouse primordial germ cells, rapid DNA demethylation occurs (Reik, 2007) and the heterochromatin markers H3K9me3 and H3K27me3 disappear (Hajkova et al., 2008) by embryonic day (E) 11.5-12.5. Similarly,

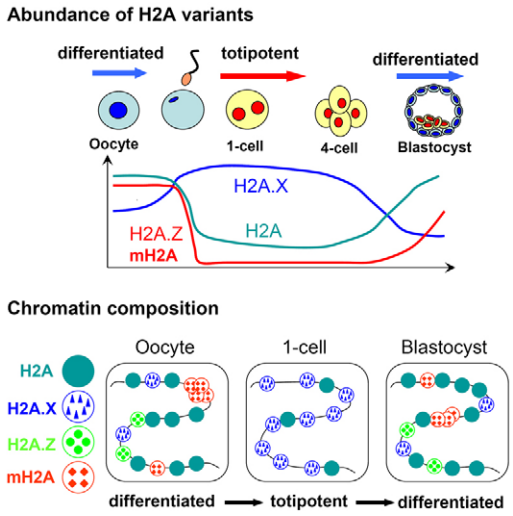

Fig. 9. Schematics of histone variant nuclear abundance and chromatin composition. In differentiated oocytes, chromatin contains the canonical histone H2A and its variants H2A.X, H2A.Z and macroH2A (mH2A). However, after fertilization, the quantity of H2A in the nucleus decreases, and H2A.Z and macroH2A almost disappear, whereas the amount of H2A.X increases. Thus, chromatin mostly contains H2A.X during the early pre-implantation stage; the embryos are totipotent and genome reprogramming occurs. At the late pre-implantation stage, when differentiation begins to occur, H2A and variant histones reappear in the nucleus, and the chromatin again contains all the histone H2A species.

active DNA demethylation occurs in the paternal genome upon fertilization (Morgan et al., 2005). H3K9me3 is absent from the paternal genome of zygotes, and H3K27me3 does not appear until the late one-cell stage (Santos et al., 2005). Recent mouse germ line studies have revealed that by E11.5, linker histone H1 is lost and chromatin is loosened, suggesting the occurrence of changes in chromatin structure (Hajkova et al., 2008). In the oocytes, oocyte-specific linker histone, H1oo (H1foo – Mouse Genome Informatics), is expressed and is replaced by the somatic linker histone after the two-cell stage (Gao et al., 2004). Finally, it should be noted that concomitant loss of histone H2A.Z and macroH2A is observed by E11.5-E12.5 (Hajkova et al., 2008). In the present study, we provided the first evidence that H2A.Z is lost from the nucleus by the late one-cell stage and confirmed a previous report that macroH2A is also removed from zygotes (Chang et al., 2005). Therefore, these epigenetic changes, which occur similarly during gametogenesis and embryogenesis, might have parallel roles in the reprogramming processes during these periods.

In many organisms, H2A.Z is essential for survival; however, it is not important for early embryonic development. In mice, H2A.Z-deficient embryos develop normally until implantation (Faast et al., 2001). In *Xenopus*, the incorporation of H2A.Z into chromatin is not observed until gastrulation (Ridgway et al., 2004). In our study, we found that H2A.Z was re-expressed at detectable levels from the late blastocyst stage when differentiation takes place. Triple staining with anti-Oct3/4 showed much higher deposition of H2A.Z in the nuclei of differentiated trophectoderm cells than in those of pluripotent inner cells (see Fig. S4 in the supplementary material). Recently, Creyghton et al. (Creyghton et al., 2008) demonstrated that H2A.Z is not required for the maintenance of undifferentiated embryonic stem (ES) cells, but is important for lineage commitment during differentiation. Thus, we suggest that H2A.Z is re-expressed in embryos when it is required to fulfill a specific function related to differentiation. Furthermore, we have shown that the nuclear incorporation of H2A.Z fused to the C-terminal 23 amino acids of H2A.X at the early pre-implantation stage causes a delay in development (Fig. 8), suggesting that the presence of H2A.Z at this stage is detrimental to pre-implantation development.

Our data suggest that chromatin in early pre-implantation embryos is enriched with H2A.X, although the canonical H2A is predominant in most somatic cells. In the immunocytochemistry studies, a strong H2A.X signal was observed in early pre-implantation embryos (Fig. 5A), whereas only low levels of canonical H2A, H2A.Z and macroH2A were detected (Fig. 1A and Fig. 3A) (Chang et al., 2005). It is impossible to compare the actual amounts of these proteins using the immunocytochemistry results, because the antibody specificities and titers used in these experiments were different. However, mRNA microinjection experiments also showed that the nuclear-incorporated Flag-H2A.X signal was much higher than those of other histone variants (Fig. 1C, Fig. 3C, Fig 4B, Fig. 5B). Because the Flag antibody was used to detect all these proteins, it was certain that the amount of incorporated H2A.X was much higher than those of other proteins. The replacement of H2A on chromatin is very fast: ~10% of the protein is replaced in 20 minutes (Higashi et al., 2007). Therefore, the levels of incorporation would reflect those of deposition in the nucleus, suggesting that H2A.X is abundant in the nuclei of early pre-implantation embryos.

H2A.X abundance in chromatin might be coincident with the proliferating and undifferentiated states of cells. H2A.X is highly conserved throughout evolution (Redon et al., 2002). In most mammalian cells, H2A.X accounts for only ~10% of the total H2A content (Mannironi et al., 1989; Rogakou et al., 1998). However, in lower eukaryotes, most H2A occurs in the form of H2A.X. In *Giardia* (highly primitive eukaryotes), the canonical histone H2A is replaced by H2A.X (Malik and Henikoff, 2003; Redon et al., 2002). In fungi, the major H2A proteins are more similar to the mammalian H2A.X variant than to the canonical H2A (Kamakaka and Biggins, 2005). Furthermore, in *Tetrahymena thermophila*, nearly half of H2A is H2A.X (Malik and Henikoff, 2003). Thus, in undifferentiated unicellular organisms, H2A.X is the predominant H2A protein. When evolution proceeded to multicellular organisms, H2A.X was replaced with H2A, and other histone variants appeared to change the chromatin structure, perhaps making it possible to regulate gene expression through more complicated mechanisms to support development of the differentiated state. Early embryos might maintain an undifferentiated state by retaining a prototype chromatin composition, i.e. H2A.X-enriched chromatin. In addition, there are some cell types in mammals that contain large amounts of H2A.X. In human SF268 astrocytoma cells, the total H2A content comprises ~25% H2A.X (Rogakou et al., 1998). In undifferentiated mouse ES cells, H2A.X is abundant and the level decreases with differentiation (Shechter et al., 2009). Taken together with our findings that H2A.X is also present at high levels in early pre-implantation embryos, abundant H2A.X might be involved in the maintenance of proliferating and undifferentiated states in higher eukaryotes.

In conclusion, chromatin deposition of histone variants changes dynamically during pre-implantation development. A summary of these changes and possible chromatin compositions are shown in Fig. 9. Formation of a unique chromatin structure as a result of the active incorporation (H2A.X) and elimination (H2A, H2A.Z and macroH2A) of particular variants seems to facilitate the reprogramming event. Notably, a lack of epigenetic markers of active or inactive genes at the early pre-implantation stage because

of a lack of H2A.Z or macroH2A and an abundance of H2A.X in the chromatin might be involved in establishing and maintaining totipotency and the high plasticity necessary for genome reprogramming.

Acknowledgements
This work was supported, in part, by Grants-in-Aid (to F.A.) from the Ministry of Education, Culture, Sports, Science and Technology of Japan (20062002).

Competing interests statement
The authors declare no competing financial interests.

Supplementary material
Supplementary material for this article is available at
http://dev.biologists.org/lookup/suppl/doi:10.1242/dev.051805/-/DC1

References

Allis, C. D., Glover, C. V., Bowen, J. K. and Gorovsky, M. A. (1980). Histone variants specific to the transcriptionally active, amitotically dividing macronucleus of the unicellular eucaryote, Tetrahymena thermophila. *Cell* **20**, 609-617.
Angelov, D., Molla, A., Perche, P. Y., Hans, F., Cote, J., Khochbin, S., Bouvet, P. and Dimitrov, S. (2003). The histone variant macroH2A interferes with transcription factor binding and SWI/SNF nucleosome remodeling. *Mol. Cell* **11**, 1033-1041.
Ausio, J. (2006). Histone variants-the structure behind the function. *Brief Funct. Genomic. Proteomic.* **5**, 228-243.
Bernstein, E. and Hake, S. B. (2006). The nucleosome: a little variation goes a long way. *Biochem. Cell Biol.* **84**, 505-517.
Brickner, D. G., Cajigas, I., Fondufe-Mittendorf, Y., Ahmed, S., Lee, P. C., Widom, J. and Brickner, J. H. (2007). H2A.Z-mediated localization of genes at the nuclear periphery confers epigenetic memory of previous transcriptional state. *PLoS Biol.* **5**, e81.
Chadwick, B. P. and Willard, H. F. (2001). Histone H2A variants and the inactive X chromosome: identification of a second macroH2A variant. *Hum. Mol. Genet.* **10**, 1101-1113.
Chang, C. C., Ma, Y., Jacobs, S., Tian, X. C., Yang, X. and Rasmussen, T. P. (2005). A maternal store of macroH2A is removed from pronuclei prior to onset of somatic macroH2A expression in preimplantation embryos. *Dev. Biol.* **278**, 367-380.
Costanzi, C. and Pehrson, J. R. (1998). Histone macroH2A1 is concentrated in the inactive X chromosome of female mammals. *Nature* **393**, 599-601.
Creyghton, M. P., Markoulaki, S., Levine, S. S., Hanna, J., Lodato, M. A., Sha, K., Young, R. A., Jaenisch, R. and Boyer, L. A. (2008). H2AZ is enriched at polycomb complex target genes in ES cells and is necessary for lineage commitment. *Cell* **135**, 649-661.
Dimitrov, S., Dasso, M. C. and Wolffe, A. P. (1994). Remodeling sperm chromatin in Xenopus laevis egg extracts: the role of core histone phosphorylation and linker histone B4 in chromatin assembly. *J. Cell Biol.* **126**, 591-601.
Faast, R., Thonglairoam, V., Schulz, T. C., Beall, J., Wells, J. R., Taylor, H., Matthaei, K., Rathjen, P. D., Tremethick, D. J. and Lyons, I. (2001). Histone variant H2A.Z is required for early mammalian development. *Curr. Biol.* **11**, 1183-1187.
Fernandez-Capetillo, O., Lee, A., Nussenzweig, M. and Nussenzweig, A. (2004). H2AX: the histone guardian of the genome. *DNA Rep.* **3**, 959-967.
Fulka, H., St John, J. C., Fulka, J. and Hozak, P. (2008). Chromatin in early mammalian embryos: achieving the pluripotent state. *Differentiation* **76**, 3-14.
Gao, S., Chung, Y. G., Parseghian, M. H., King, G. J., Adashi, E. Y. and Latham, K. E. (2004). Rapid H1 linker histone transitions following fertilization or somatic cell nuclear transfer: evidence for a uniform developmental program in mice. *Dev. Biol.* **266**, 62-75.
Graves, R. A., Marzluff, W. F., Giebelhaus, D. H. and Schultz, G. A. (1985). Quantitative and qualitative changes in histone gene expression during early mouse embryo development. *Proc. Natl. Acad. Sci. USA* **82**, 5685-5689.
Hajkova, P., Ancelin, K., Waldmann, T., Lacoste, N., Lange, U. C., Cesari, F., Lee, C., Almouzni, G., Schneider, R. and Surani, M. A. (2008). Chromatin dynamics during epigenetic reprogramming in the mouse germ line. *Nature* **452**, 877-881.
Hamatani, T., Carter, M. G., Sharov, A. A. and Ko, M. S. (2004). Dynamics of global gene expression changes during mouse preimplantation development. *Dev. Cell* **6**, 117-131.
Higashi, T., Matsunaga, S., Isobe, K., Morimoto, A., Shimada, T., Kataoka, S., Watanabe, W., Uchiyama, S., Itoh, K. and Fukui, K. (2007). Histone H2A mobility is regulated by its tails and acetylation of core histone tails. *Biochem. Biophys. Res. Commun.* **357**, 627-632.
Inoue, A. and Aoki, F. (2010). Role of the nucleoplasmin 2 C-terminal domain in the formation of nucleolus-like bodies in mouse oocytes. *FASEB J.* **24**, 485-494.
Jin, C., Zang, C., Wei, G., Cui, K., Peng, W., Zhao, K. and Felsenfeld, G. (2009). H3.3/H2A.Z double variant-containing nucleosomes mark 'nucleosome-free regions' of active promoters and other regulatory regions. *Nat. Genet.* **41**, 941-945.
Kageyama, S., Liu, H., Kaneko, N., Ooga, M., Nagata, M. and Aoki, F. (2007). Alterations in epigenetic modifications during oocyte growth in mice. *Reproduction* **133**, 85-94.
Kamakaka, R. T. and Biggins, S. (2005). Histone variants: deviants? *Genes Dev.* **19**, 295-310.
Kimmins, S. and Sassone-Corsi, P. (2005). Chromatin remodelling and epigenetic features of germ cells. *Nature* **434**, 583-589.
Kimura, H. and Cook, P. R. (2001). Kinetics of core histones in living human cells: little exchange of H3 and H4 and some rapid exchange of H2B. *J. Cell Biol.* **153**, 1341-1353.
Liu, H., Kim, J. M. and Aoki, F. (2004). Regulation of histone H3 lysine 9 methylation in oocytes and early pre-implantation embryos. *Development* **131**, 2269-2280.
Loyola, A., Bonaldi, T., Roche, D., Imhof, A. and Almouzni, G. (2006). PTMs on H3 variants before chromatin assembly potentiate their final epigenetic state. *Mol. Cell* **24**, 309-316.
Malik, H. S. and Henikoff, S. (2003). Phylogenomics of the nucleosome. *Nat. Struct. Biol.* **10**, 882-891.
Mannironi, C., Bonner, W. M. and Hatch, C. L. (1989). H2A.X. a histone isoprotein with a conserved C-terminal sequence, is encoded by a novel mRNA with both DNA replication type and polyA 3' processing signals. *Nucleic Acids Res.* **17**, 9113-9126.
Marzluff, W. F., Gongidi, P., Woods, K. R., Jin, J. and Maltais, L. J. (2002). The human and mouse replication-dependent histone genes. *Genomics* **80**, 487-498.
Meneghini, M. D., Wu, M. and Madhani, H. D. (2003). Conserved histone variant H2A.Z protects euchromatin from the ectopic spread of silent heterochromatin. *Cell* **112**, 725-736.
Morgan, H. D., Santos, F., Green, K., Dean, W. and Reik, W. (2005). Epigenetic reprogramming in mammals. *Hum. Mol. Genet.* **14 Suppl. 1**, R47-R58.
Niwa, H., Yamamura, K. and Miyazaki, J. (1991). Efficient selection for high-expression transfectants with a novel eukaryotic vector. *Gene* **108**, 193-199.
Ohsumi, K. and Katagiri, C. (1991). Occurrence of H1 subtypes specific to pronuclei and cleavage-stage cell nuclei of anuran amphibians. *Dev. Biol.* **147**, 110-120.
Pusarla, R. H. and Bhargava, P. (2005). Histones in functional diversification. Core histone variants. *FEBS J.* **272**, 5149-5168.
Rangasamy, D., Berven, L., Ridgway, P. and Tremethick, D. J. (2003). Pericentric heterochromatin becomes enriched with H2A.Z during early mammalian development. *EMBO J.* **22**, 1599-1607.
Rasmussen, T. P., Huang, T., Mastrangelo, M. A., Loring, J., Panning, B. and Jaenisch, R. (1999). Messenger RNAs encoding mouse histone macroH2A1 isoforms are expressed at similar levels in male and female cells and result from alternative splicing. *Nucleic Acids Res.* **27**, 3685-3689.
Redon, C., Pilch, D., Rogakou, E., Sedelnikova, O., Newrock, K. and Bonner, W. (2002). Histone H2A variants H2AX and H2AZ. *Curr. Opin. Genet. Dev.* **12**, 162-169.
Reik, W. (2007). Stability and flexibility of epigenetic gene regulation in mammalian development. *Nature* **447**, 425-432.
Ridgway, P., Brown, K. D., Rangasamy, D., Svensson, U. and Tremethick, D. J. (2004). Unique residues on the H2A.Z containing nucleosome surface are important for Xenopus laevis development. *J. Biol. Chem.* **279**, 43815-43820.
Rogakou, E. P., Pilch, D. R., Orr, A. H., Ivanova, V. S. and Bonner, W. M. (1998). DNA double-stranded breaks induce histone H2AX phosphorylation on serine 139. *J. Biol. Chem.* **273**, 5858-5868.
Santenard, A. and Torres-Padilla, M. E. (2009). Epigenetic reprogramming in mammalian reproduction: contribution from histone variants. *Epigenetics* **4**, 80-84.
Santos, F. and Dean, W. (2004). Epigenetic reprogramming during early development in mammals. *Reproduction* **127**, 643-651.
Santos, F., Peters, A. H., Otte, A. P., Reik, W. and Dean, W. (2005). Dynamic chromatin modifications characterise the first cell cycle in mouse embryos. *Dev. Biol.* **280**, 225-236.
Shechter, D., Chitta, R. K., Xiao, A., Shabanowitz, J., Hunt, D. F. and Allis, C. D. (2009). A distinct H2A.X isoform is enriched in Xenopus laevis eggs and early embryos and is phosphorylated in the absence of a checkpoint. *Proc. Natl. Acad. Sci. USA* **106**, 749-754.
van der Heijden, G. W., Dieker, J. W., Derijck, A. A., Muller, S., Berden, J. H., Braat, D. D., van der Vlag, J. and de Boer, P. (2005). Asymmetry in histone H3 variants and lysine methylation between paternal and maternal chromatin of the early mouse zygote. *Mech. Dev.* **122**, 1008-1022.
Wassarman, P. M. and Mrozak, S. C. (1981). Program of early development in the mammal: synthesis and intracellular migration of histone H4 during oogenesis in the mouse. *Dev. Biol.* **84**, 364-371.
Yamagata, K. (2008). Capturing epigenetic dynamics during pre-implantation development using live cell imaging. *J. Biochem.* **143**, 279-286.
Zlatanova, J. and Thakar, A. (2008). H2A.Z: view from the top. *Structure* **16**, 166-179.